Chinese Chemical Letters 33 (2022) 2617–2620

Contents lists available at ScienceDirect

Chinese Chemical Letters

journal homepage: www.elsevier.com/locate/cclet

Keggin-type polycationic $AlO_4Al_{12}(OH)_{24}(H_2O)_{12}^{7+}$ intercalated MoO_3 composites for methyl orange adsorption

Qian Wang[a,1], Hongrui Tian[b,1], Zhong Zhang[a], Tianyi Dang[a], Wanyu Zhang[a], Jie Wang[a], Ying Lu[a], Shuxia Liu[a,*]

[a] Key Laboratory of Polyoxometalate and Reticular Material Chemistry of the Ministry of Education, College of Chemistry, Northeast Normal University, Changchun 130024, China
[b] Department of Chemistry and Shenzhen Grubbs Institute, Southern University of Science and Technology, Shenzhen 518055, China

ARTICLE INFO

Article history:
Received 2 September 2021
Revised 20 September 2021
Accepted 23 September 2021
Available online 29 September 2021

Keywords:
MoO_3
Keggin-type polycationic
$AlO_4Al_{12}(OH)_{24}(H_2O)_{12}^{7+}$
Intercalation
Adsorption
Methyl orange dye

ABSTRACT

Molybdenum trioxide (MoO_3) can be employed as an excellent host for intercalation due to its 2D layered structure that connected by van der Waals interactions. Herein, a series of polyoxometalate-based MoO_3 composites (Al_{13}@MoO_3) were successfully prepared by interpolating the Keggin-type polycationic $AlO_4Al_{12}(OH)_{24}(H_2O)_{12}^{7+}$ (Al_{13}) into MoO_3 gallery. These composites can be applied to rapidly adsorb the anionic dye methyl orange (MO) through strong electrostatic interactions lead to compact and stable gathering in the surrounding of the numerous charged Al_{13}. Adsorption behaviors of composites with the different amount of Al_{13} were determined, these results revealed that Al_{13}-3.34%@MoO_3 exhibited the most remarkable adsorption capacity. More importantly, the composite maintains superior adsorption capacity for five consecutive adsorption/desorption cycles, suggesting that Al_{13}@MoO_3 can be an efficient and durable adsorbent.

Methyl orange (MO) is a kind of azobenzene sulfonic acid dyes with complex aromatic ring, which can cause considerable damage to human health originated from carcinogenic and mutagenic effects. In recent years, a wide variety of methods have been employed to remove MO such as chemical oxidation [1], degradation [2,3], membrane separation [4], ion exchange [5] and adsorption [6,7]. Among these methods, the adsorption-based process is one of the most favorable approach strategies in terms of versatility, simplicity, promptness, and efficiency. Traditional adsorbent like activated carbon faces poor efficiency and expensive price issues [8]. Currently, novel generation materials are considered as excellent adsorbents, including zeolites [9], functionalized clays [10] and some composite materials [11]. Within these substances, intercalation composites are emerging as promising adsorbent materials due to their potential advantages, including well-ordered layered structure, larger gallery space and controllability of interlayer species [12].

MoO_3 is a 2D layered structure with covalently bonded oxide layers separated by van der Waals interactions [13]. In some cases, the 2D layered structure of the host lattice can slack as guest species are immobilized, forming intercalation materials with extension of the interlayer separation. In the previous works, small molecules such as acrylamide [14], nicotinamide [15] can be introduced into MoO_3 under room temperature stirring, while larger molecules cannot be inserted diametrically. A method is proposed that MoO_3 can be reduced to $[Na(H_2O)_2]_xMoO_3$ using for ion exchange based on $Na(H_2O)_2^+$ is replaced by macromolecular to achieve intercalation [16–19]. For example, Nazar *et al.* utilized Al_{13} to exchange $Na(H_2O)_2^+$ further to obtain Al_{13} pillared microporous MoO_3 hybrid materials, the gallery spacing enlarged to 17.35 Å [20]. However, the combination process of $[Na(H_2O)_2]_xMoO_3$ has been protected under N_2 and sample deposits in N_2 dry-box [21]. Surprisingly, Pan took a simple and convenient strategy directly to interpolate different lengths alkylamine into MoO_3 layers [22]. Among them, MoO_3 intercalation material (MoO_3-DDA) through introducing dodecylamine (DDA) into MoO_3 improves the interval from 6.9 Å to 30.86 Å, and the larger space area is more conducive to import other guest molecules, which provides an exceptional technology for the preparation of intercalation composites.

Polyoxometalates (POMs), as one kind of significant metal-oxide clusters with multiple charge have been employed in dyeadsorption [23,24]. Regrettably, the high solubility in aqueous solution cannot realize selective separation and reuse. A series of outstanding works have been executed to incorporate

* Corresponding author.
E-mail address: liusx@nenu.edu.cn (S. Liu).
[1] These authors contributed equally to this work.

https://doi.org/10.1016/j.cclet.2021.09.079
1001-8417/

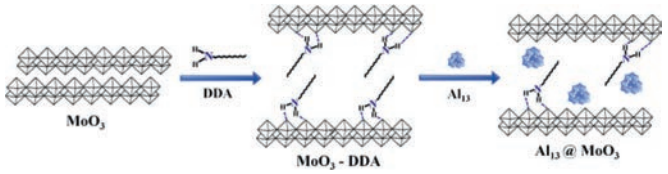

Scheme 1. Preparation methods of MoO_3-DDA and Al_{13}@MoO_3.

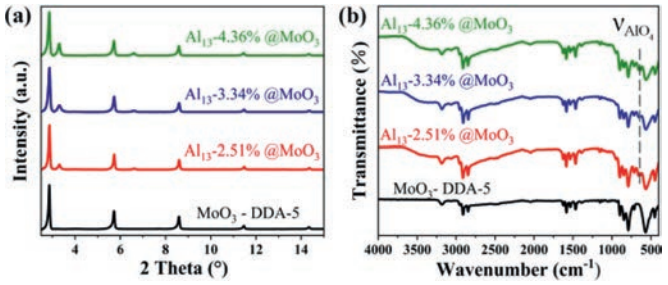

Fig. 1. MoO_3-DDA-5 and Al_{13}@MoO_3 with different Al_{13} con-centration: (a) PXRD patterns. (b) FT-IR spectra.

POMs into layered compounds to prepare POMs-based intercalation composites [25,26]. For example, Lesbani *et al.* introduced $[\alpha\text{-}PW_{12}O_{40}]^{3-}$ into Mg/Fe layered double hydroxides (LDH) host, extremely improved Cd^{2+} adsorption [27]. Similarly, Xu *et al.* reported $[P_2W_{17}]^{10-}$ and $[CoW_{12}]^{5-}$ intercalated ZnAlFe LDH, which could enrich with the adsorption function for cationic dye methylene blue [28]. Despite above progress achieved, cationic POMs like $AlO_4Al_{12}(OH)_{24}(H_2O)_{12}^{7+}$ (Al_{13}) as guest to construct intercalation composites suffer setbacks, searching for an advisable host encapsulate cationic POMs as an imaginative point.

Herein, we successfully prepared a series of Al_{13}@MoO_3 composites with different Al_{13} loading by implanting Al_{13} guests into extensive airspace of MoO_3-DDA-5 which the molar ratio of DDA to MoO_3 is 5, as shown in Scheme 1. These composites demonstrate a certain adsorption capacity for MO due to the electrostatic interaction effects between cation Al_{13} and anion MO. Among these, Al_{13}-3.34%@MoO_3 exhibits superior performance with the rate up to 93% in 20 min as well as adsorption capacity to 357.2 mg/g, which is a useful adsorption material to eliminate MO.

MoO_3-DDA-5 hybrid was synthesized by the literature method [22] and indicated 30.89 Å separation interstice (Fig. S1a in Supporting information). The van der Waals diameter of Al_{13} cluster is 10.5 Å [20], therefore, it can migrate into the MoO_3-DDA-5 passageway through the capillary phenomenon. Furthermore, replacement of Al_{13} solution each 24 h results in Al_{13} embedding easily in MoO_3-DDA-5 thoroughfare derived from concentration disparity between inside and outside of the layer. Subsequently, Al_{13}@MoO_3 composites with diverse Al_{13} concentration are prepared, denoted as Al_{13}-2.51%@MoO_3, Al_{13}-3.34%@MoO_3, Al_{13}-4.36%@MoO_3, respectively.

The PXRD patterns indicated that Al_{13}@MoO_3 appeared new characteristic diffraction peaks at $2\theta = 3.30°$ and $2\theta = 6.60°$ compared with MoO_3-DDA-5 (Fig. 1a). Layer spacing can be calculated by $2d\sin\theta = n\lambda$, the consequent of 26.77 Å is narrower than 30.89 Å of MoO_3-DDA-5. The variability of layer interspace could be associated with introduction of Al_{13} due to the diameter of Al_{13} is smaller than DDA molecular size. It is worth noting that Al_{13}@MoO_3 exhibit two spacings of 30.89 Å and 26.77 Å, which corroborated incompletely deintercalated for DDA molecules. In addition, sharp peaks gradually enhance at 3.30° and 6.60° with increasing of immersion time, which can probably be attributed to the improved content of Al_{13}.

The FT-IR spectra of Al_{13}@MoO_3 composites were obtained in the range of 4000-400 cm^{-1} (Fig. 1b). Al_{13}@MoO_3 composites exhibit a new characteristic peak at 630 cm^{-1}, which is attributed to the AlO_4 symmetric stretching vibration peak, and the characteristic peak at 3700–3400 cm^{-1} correspond to the stretching vibration of the –OH on the Al_{13} cluster surface [29], further verified that Al_{13} is successfully encapsulated into MoO_3-DDA.

To further explore the morphology of composites, scanning electron microscope (SEM) images were observed, as shown in Figs. S4a–e (Supporting information). MoO_3-DDA-5 exhibits a special uniform flake morphology and smooth surface, but the size significantly shrinks than MoO_3. The morphology of Al_{13}@MoO_3 composites gradually changed. Due to immersing time influence of Al_{13}, Al_{13}@MoO_3 appear cracks and holes. To define the content of elements in the Al_{13}@MoO_3 composites, energy dispersive spectroscopy (EDS) experiment was determined (Fig. S5 in Supporting information), suggesting that the weight percentages of Al in the three composites were 2.28 wt%, 2.93 wt% and 3.50 wt%, respectively. It is worth noting that the content of Al_{13} is proportional with immersion time. The same conclusion can be further confirmed by elemental analyses (Table S1 in Supporting information). The elements of Mo, Al, C, N and O in Al_{13}-3.34%@MoO_3 were corroborated by element X-ray mapping as shown in Fig. S4 (Supporting information), indicating Al and other elements are uniformly distributed on this composite.

We choose the typical anionic dye MO as the research substance to assess the capacity of these composites. Considering that MoO_3 and MoO_3-DDA-5 also have ordered layer structures could accommodate pollutant, we investigated the adsorption performance for MO. The adsorption curves indicate that MoO_3 shows unobvious adsorption capacity (Fig. S7a in Supporting information), while MoO_3- DDA-m (m represents the molar ratio of DDA to MoO_3, m = 1, 2, 3, 4, 5) composites exhibit a little bit better adsorption behavior (Figs. S7b and f in Supporting information). We found that the amount of adsorbed MO increased as the ratios of DDA raised from 1 up to 5, reaching the adsorption rate value of 82% after 20 min by MoO_3-DDA-5 (Fig. S7f). The possible reason for the different adsorption behaviors is that layer distance with accommodating MO has impact on capability. The above completion leads to MoO_3-DDA-5 is selected as intercalation target for the immersing of Al_{13}.

Owing to the electrostatic attraction exist between Al_{13} and anionic MO. We further studied the adsorption properties of Al_{13}@MoO_3 (Fig. 2a). Expectantly, the results manifest that the adsorption ability enhanced with the amount of Al_{13} less than 3.34%, the rate value of Al_{13}-3.34%@MoO_3 reach 61% within 1 min, 87.3% after 5 min, attaining 93% after 20 min as adsorption equilibrium already appeared, exhibiting impressive ability toward quickly remove MO. However, with the amount of Al_{13} above 3.34%, the adsorption rate and adsorption capacity of Al_{13}@MoO_3 composites initiate to decrease unexpectedly (Fig. 2b, Figs. S7c-e in Supporting information). The possible reason for the above phenomenon is believed to be that strong electrostatic interaction [30,31] between Al_{13} with highly positive charges and anionic dye MO is propitious to absorb MO, which is incarnated on the raising adsorbed amount of MO as the content of Al_{13} below 3.34%. With the amount of Al_{13} further increased, excessive Al_{13} will occupy the original internal area of Al_{13}@MoO_3 for accommodating MO dye, and the remaining space is inadequate to effectively encase much number of MO molecules, so that the adsorption capacity declined.

In addition, the adsorption capacity of Al_{13}@MoO_3 composites are investigated by the 100 mg/L concentration of MO dye (Fig. 2c), suggesting that the adsorption capacities of composites are 320.6 mg/g, 357.2 mg/g and 295.1 mg/g after 2 h, respectively. We found that the amount of MO adsorption at the beginning get better with the increase of Al_{13} loading, then decreases, the consequent

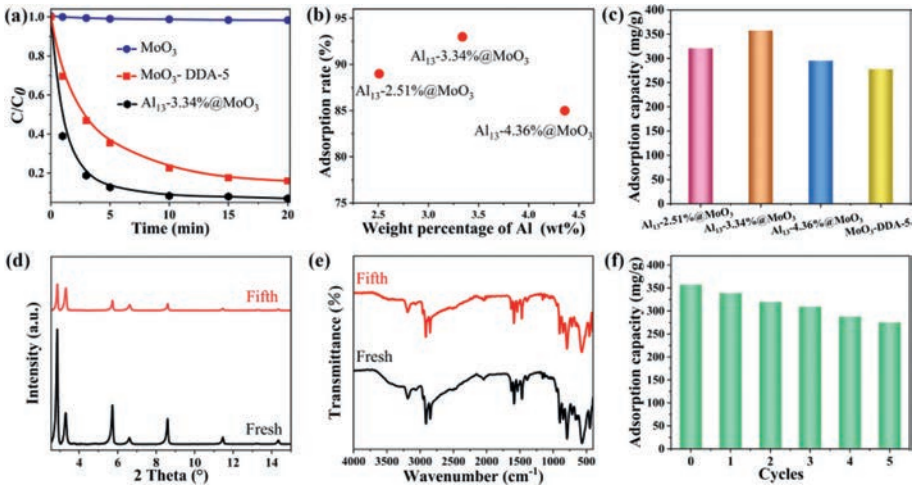

Fig. 2. (a) The concentration changes of MO at different times (Adsorbent: 40 mg, MO initial concentration: 20 mg/L, volume: 40 mL). (b) Adsorption rate of MO with Al_{13}@MoO_3 after 20 min (Al content measured by ICP). (c) Absorption capacity of Al_{13}@MoO_3 and MoO_3-DDA-5 (Adsorbent: 10 mg, MO concentration: 100 mg/L, volume: 100 mL). Al_{13}-3.34%@MoO_3 fresh and after five cycles: (d) PXRD patterns, (e) FT-IR spectra, (f) Absorption capacity. (Adsorbent: 10 mg, MO concentration: 100 mg/L, volume: 100 mL).

Table 1
The adsorption capacities of different adsorbents.

Adsorbents	Adsorption capacity (mg/g)	References
Nanoporous carbon	18.8	[32]
Co-MOF	20	[33]
rGO/Ni/MMO	84.2	[34]
PANI–Co_3O_4	107	[35]
Chitosan/PVA/zeolite	153	[36]
SiO_2@LDH	166.1	[37]
10% GO/MIL-101 (Fe)	186.2	[38]
70% SA-MIL-101	291.5	[39]
Al_{13}-3.34%@MoO_3	357.2	This work

is in fair agreement with the previous adsorption behavior. Compared with other adsorbents previously reported in the literature, Al_{13}-3.34%@MoO_3 composites have higher MO adsorption capacity value (Table 1) [32–39].

We have selected the material with the best adsorption effect to investigate its regeneration ability, PXRD patterns and FT-IR spectra indicate that the recycled adsorbent is consistent with fresh material (Figs. 2d and e), the conclusion can be comprehended in terms of a recyclable material. The experiment result of the adsorption capacity for revived Al_{13}-3.34%@MoO_3 indicates the amount of adsorbed MO decreased slightly (Fig. 2f), which is attributed to the loss of Al_{13} existing amid interlayers during multiple washing process.

In summary, we successfully prepared Al_{13}@MoO_3 intercalation composites by encapsulating polycationic Al_{13} clusters into MoO_3 layers area. These composites are utilized to evaluate the adsorption capacity of MO due to the electrostatic attraction interaction between cation Al_{13} and anionic MO. The adsorption results show that Al_{13}-3.34%@MoO_3 is provided with the noticeable amounts of MO adsorption capacity as 357.2 mg/g and the rapid rate reaches 93% after 20 min. Recycling experiments illustrate that the structure is pristine during the adsorption process, exhibiting favorable stability to MO removing.

Declaration of competing interest

The authors declare that they have no known competing financial interests or personal relationships that could have appeared to influence the work reported in this paper.

Acknowledgment

The authors thank the National Natural Science Foundation of China (Nos. 21872021, 21671033, 22172022 and 22071019).

Supplementary materials

Supplementary material associated with this article can be found, in the online version, at doi:10.1016/j.cclet.2021.09.079.

References

[1] P.H. Shao, X.G. Duan, J. Xu, et al., J. Hazard. Mater. 322 (2017) 532–539.
[2] W.C. Huang, L.M. Lyu, Y.C. Yang, et al., J. Am. Chem. Soc. 134 (2012) 1261–1267.
[3] Y.N. Liu, F. Zhang, J. Li, et al., Environ. Sci. Technol. 51 (2017) 8616–8623.
[4] S.Y. Fang, P. Zhang, J.L. Gong, et al., Chem. Eng. J. 385 (2020) 123400.
[5] W. Yao, S.J. Yu, J. Wang, et al., Chem. Eng. J. 307 (2017) 476–486.
[6] M.D. Faysal Hossain, N. Akther, Y.B. Zhou, Chin. Chem. Lett. 31 (2020) 2525–2538.
[7] R.M. Yu, Y.Z. Shi, D.Z. Yang, et al., ACS Appl. Mater. Interfaces 9 (2017) 21809–21819.
[8] P. Monash, G. Pugazhenthi, Environ. Prog. Sustain. Energy 33 (2014) 154–159.
[9] S. Radoor, J. Karayil, A. Jayakumar, et al., Colloids Surf. A 611 (2021) 125852.
[10] A.M. Zayed, M.M. Abdel Wahed, E.A. Mohamed, et al., Appl. Clay Sci. 166 (2018) 49–60.
[11] H.Y. Zhu, R. Jiang, Y.Q. Fu, et al., Appl. Surf. Sci. 258 (2011) 1337–1344.
[12] Y.Q. Zheng, B. Cheng, W. You, et al., J. Hazard. Mater. 369 (2019) 214–225.
[13] M.Z. Wang, K.J. Koski, ACS Nano 9 (2015) 3226–3233.
[14] R.F. Farias, M.S. Refat, H.A. Hashem, J. Incl. Phenom. Macrocycl. Chem. 61 (2008) 113–118.
[15] F. Robson, Mater. Chem. Phys. 90 (2005) 302–309.
[16] H. Tagaya, K. Ara, J.I. Kadokawa, et al., J. Mater. Chem. 4 (1994) 551–555.
[17] T. Itoh, J.Z. Wang, I. Matsubara, et al., Mater. Lett. 62 (2008) 3021–3023.
[18] T. Itoh, I. Matsubara, W. Shin, et al., J. Ceram. Soc. Jpn. 118 (2010) 171–174.
[19] T. Itoh, I. Matsubara, W. Shin, et al., Mater. Lett. 61 (2007) 4031–4034.
[20] L.F. Nazar, S.W. Liblong, X.T. Yin, J. Am. Chem. Soc. 113 (1991) 5889–5890.
[21] L. Wang, J. Schindler, C.R. Kannewurf, et al., J. Mater. Chem. 7 (1997) 1277–1283.
[22] Y. Jing, Q.Y. Pan, Z.X. Cheng, et al., Mater. Sci. Eng. B 138 (2007) 55–59.
[23] A.X. Yan, S.. Yao, Y.G. Li, et al., Chem. Eur. J. 20 (2014) 6927–6933.
[24] F.Y. Yi, W. Zhu, S. Dang, et al., Chem. Commun. 51 (2015) 3336.
[25] X.R. Sun, J. Dong, Z. Li, et al., Dalton Trans. 48 (2019) 5285–5291.
[26] B. Bi, L. Xu, B.B. Xu, et al., Appl. Clay Sci. 54 (2011) 242–247.
[27] A. Lesbani, D.R. Maretha, T. Taher, et al., Alp Conf. Proc. 2049 (2018) 020013.
[28] M. Xu, B. Bi, B.B. Xu, et al., Appl. Clay Sci. 157 (2018) 86–91.
[29] D.L. Teagarden, J.F. Kozlowski, J.L. White, et al., J. Pharm. Sci. 70 (1981) 758–761.
[30] Y.W. Liu, S.M. Liu, S.X. Liu, et al., Small 13 (2017) 1603174.
[31] Y.Q. Hu, T. Guo, X.S. Ye, et al., Chem. Eng. J. 228 (2013) 392–397.
[32] S. Kundu, I.H. Chowdhury, M.K. Naskar, J. Mol. Liq. 234 (2017) 417–423.
[33] Y. Deng, Y. Zhao, P. Wang, et al., Microporous Mesoporous Mater. 241 (2017) 192–201.

[34] Z. Yang, S.S. Ji, W. Gao, et al., J. Colloid Interface Sci. 408 (2013) 25–32.
[35] S. Shahabuddin, N.M. Sarih, S. Mohamad, et al., RSC Adv. 6 (2016) 43388–43400.
[36] U. Habiba, T.A. Siddique, J.J. Li Lee, et al., Carbohydr. Polym. 191 (2018) 79–85.
[37] D.X. Yang, S. Song, Y.D. Zou, et al., Chem. Eng. J. 323 (2017) 143–152.
[38] Z.N. Liu, W.W. He, Q.Y. Zhang, et al., ACS Omega 6 (2021) 4597–4608.
[39] S.A. El-Hakam, S.E. Samra, S.M. El-Dafrawy, et al., RSC Adv. 8 (2018) 20517–20533.